Spiral Constellations for Phase Noise Channels

This article has been accepted for publication in a future issue of this journal, but has not been fully edited. Content may change prior to final publication. Citation information: DOI 10.1109/TCOMM.2019.2937293, IEEE Transactions on Communications

Spiral Constellations for Phase Noise Channels

Alessandro Ugolini, Amina Piemontese, and Thomas Eriksson

***Abstract*—In this paper, we consider the design of spiral constellations for channels affected by phase noise. The strength of the proposed constellations resides both on the performance and on the extreme simplicity of the design. The symbols can in fact be expressed in analytical form, and are uniquely defined through a single parameter that accounts for the phase and thermal noise variances. The structure of the proposed constellations allows to easily determine the points that are closest to any point in the complex plane, therefore we also propose a low complexity detector that is suitable for phase noise channels in medium-high signal-to-noise ratio conditions. The performance of the proposed constellations are assessed in terms of information rate and error rate. Despite their simplicity, the new spiral constellations have excellent performance, especially when the constellation size grows large.**

***Index Terms*—Phase noise; spiral constellations; constellation design.**

I. Introduction

High order constellations represent a possible answer to the increasing demand for high datarate transmissions over bandlimited channels. However, their sensitivity to channel imperfections is a critical aspect. High order modulation schemes are susceptible, for example, to phase noise (PN), that can be considered one of the major impairments of many communication links. In most wireless communication systems, PN arises from local oscillator instabilities [1]. An example is represented by the second generation digital video broadcasting satellite (DVB-S2X) system [2], where inexpensive low-noise block downconverters are employed in the receiver outdoor unit, and introduce a strong PN. Another example is the microwave backhaul link in mobile cellular networks, where the PN introduced by the radio-frequency oscillators used at the transmitter and the receiver has a high impact on the performance [3]. Similarly, PN of the lasers at the transmitter and receiver strongly degrades the performance of long-haul optical coherent systems [4].

The problem of reaching near-coherent performance in the presence of PN has been extensively studied in the past, considering both linear and continuous-phase modulations [5]–[7]. One solution consists of adopting advanced joint detection and estimation techniques at the receiver side (e.g., see [8]–[14] and references therein). Recently, algorithms for approximate maximum likelihood detection for MIMO systems impaired by PN have been proposed in [15] and [16].

To further improve the performance, a properly designed constellation can be employed. The problem was addressed for example by Foschini *et al.* in [17] already in the early 70s. In this work, an approximate maximum likelihood detector was derived for a memoryless PN channel, and constellations that optimize its symbol error probability were obtained. More recently, in [18], constellation points are optimized by maximizing the mutual information using a simulated annealing algorithm. In [19], the problem of finding the optimal constellation for PN channel is investigated by considering optimization formulations based on error rate and mutual information. In [20], the performance of high order amplitude-phase shift keying (APSK) constellations in PN channels are compared to the conventional PSK and quadrature amplitude modulation (QAM) constellations. Spiral constellations, called spiral QAM, have been considered for PN channels in [21].

Although it has been well investigated in the past, the problem of finding a good constellation robust to PN is far from being solved. The main drawback of the design approaches in the literature is the complexity, since they require the optimization of several parameters and some of them produce unstructured constellations that lack flexibility.

In this paper, we propose new spiral constellations for PN channels, whose points are properly located along an Archimedean spiral. The choice of this particular spiral is motivated by its property of constant radial distance between spiral laps. The proposed constellations have excellent performance and are very simple to design. The constellation symbols can in fact be expressed in analytical form, and are uniquely defined through a single parameter, therefore they are very versatile. Moreover, the structure of the proposed constellation allows a very simple bit-to-symbol mapping, inspired by the QAM mapping. The main difference with respect to the work in [21] is that the design of the spirals proposed in [21] is based on a more computationally intensive process, and it does not allow for a closed form expression.

We also propose a low complexity detector based on a novel closest point search strategy that exploits the regular and simple shape of our spiral constellations. The proposed detector allows to significantly reduce the complexity of the receiver and has excellent performance in medium-high signal-to-noise ratio conditions.

We demonstrate the effectiveness of the proposed new techniques through a complete set of numerical results, taking into account different scenarios and different performance metrics. We show that the new spiral constellations allow to achieve very high information rate (IR), and have superior performance with respect to competing constellations. In particular, we compare the proposed constellations with classical QAM and APSK, and with the constellation scheme proposed in [21], which is specifically designed for PN channels.

Interestingly, the new spiral constellations are shown to be suitable for applications in practical coded systems adopting

This paper was presented in part at the IEEE Wireless Communications and Networking Conference, Marrakesh, Morocco, Apr. 2019.

A. Ugolini is with the Department of Engineering and Architecture, University of Parma, Italy (E-mail: alessandro.ugolini@unipr.it). A. Piemontese and T. Eriksson are with the Department of Electrical Engineering, Chalmers University of Technology, Gothenburg, Sweden (E-mail: aminap@chalmers.se, thomase@chalmers.se).

This article has been accepted for publication in a future issue of this journal, but has not been fully edited. Content may change prior to final publication. Citation information: DOI 10.1109/TCOMM.2019.2937293, IEEE Transactions on Communications

state-of-the-art channel codes, that is, they do not require a redesign of the channel code.

The remainder of the paper is organized as follows. The system model is introduced in Section II. The new constellations are described in Section III, while the performance metrics used to optimize them and to compare them with state-of-the-art constellations are described in Section IV. A low complexity detector is described in Section V. Section VI presents and discusses numerical results and finally some conclusions are drawn in Section VII.

II. System Model

We consider the transmission of linearly modulated symbols impaired by PN and additive white Gaussian noise (AWGN). We assume Nyquist transmitted pulses, matched filtering, and no intersymbol interference. We consider a modular receiver architecture, where channel estimation is performed before the symbol detection, and the discrete-time baseband received signal is given by

$$y_k = x_k e^{j\phi_k} + w_k \,, \tag{1}$$

where x_k is the transmitted symbol, ϕ_k is the PN sample, representing the residual PN after the phase tracking and compensation procedure, and w_k is a complex AWGN term, with variance σ_w^2. For the PN, we assume that the samples $\{\phi_k\}$ have a zero-mean Gaussian distribution with variance σ_ϕ^2, a reasonable assumption when PN has been tracked by resorting, for example, to pilot symbols [19]. In general, the residual PN samples may be correlated, however, in order to simplify the analysis, we assume that an ideal estimator is used that removes any correlation [15], [17], [19]. Therefore, the residual PN sequence represents a memoryless phase noise process [22]. The transmitted symbols are possibly obtained from the encoding of a sequence of information symbols by means of a code $\mathcal{C}$. We assume that the symbol x_k is drawn from an M-point signal constellation $\{c_m, m \in \{1, \ldots, M\}\}$ and that all the constellation points are transmitted with equal probability $1/M$. Our goal is to design constellations of order M, whose points are placed along an Archimedean spiral. The approach used to find good constellations is described in Section IV and is based on the maximization of the achievable and of the pragmatic IR.

III. Spiral Constellations Design

In this section, we describe the proposed spiral constellations. An Archimedean spiral is defined by the following equation

$$s(t) = te^{jt} \,. \tag{2}$$

We propose to place the constellation points along the spiral, according to the following rule,

$$c_m = t_m e^{jt_m} \quad m = 1, \ldots, M \,, \tag{3}$$

where M is the cardinality of the desired constellation and $t_1 < t_2 < \ldots < t_M$. In the following, we describe how to choose the parameters t_m. We first consider the AWGN case, then we describe the construction in the case of PN. We define

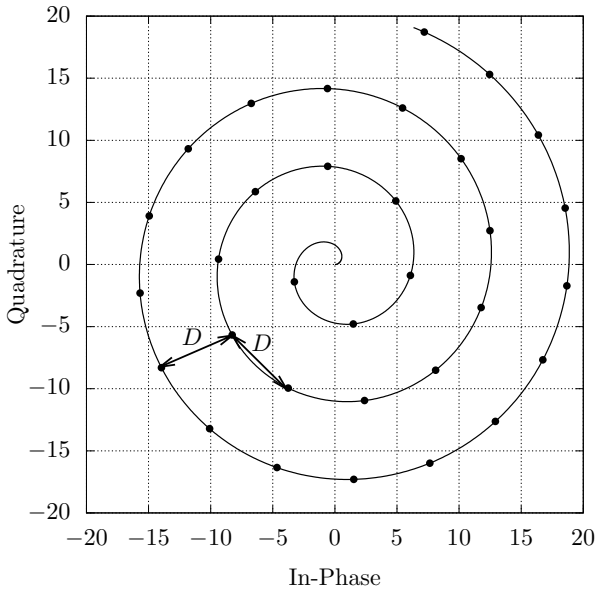

Figure 1. Spiral constellation with $M = 32$ points.

as D_m the distance between two consecutive points on a spiral expressed by (3):

$$D_m = |c_{m+1} - c_m| \,. \tag{4}$$

A. Spiral Constellations for the AWGN Channel

Since asymptotic performance on the AWGN channel depends on the minimum distance of the adopted constellation [23], a good way to place constellation points on a spiral when the only impairment is AWGN is to choose the points regularly along the spiral, so that the distance between consecutive symbols is the same. With this aim, we formulate the equation for the constellation points as explained by the following theorem.

Theorem 1. *If we place constellation points on the spiral according to the equation $t_m = \sqrt{2Dm}$, we will get a distance between consecutive points that is approximately equal to D, for all points. If we set $D = 2\pi$, the consecutive laps of the spiral are at the same distance D as the points along the spiral.*

Proof: see Appendix A.

Fig. 1 shows with the solid line the Archimedean spiral (2), and with the circles a spiral constellation with $M = 32$ points, built according to the design specified by Theorem 1. In the figure, we have highlighted that the distance between two consecutive points and that between two consecutive laps are approximately the same and equal to $D = 2\pi$. The constellation points are then normalized such that the resulting constellation has unitary energy.

B. Spiral Constellations in Phase Noise

We extend the construction of a spiral constellation to take into account the presence of PN. The proposed construction is based on the observation that the PN affects more severely

This article has been accepted for publication in a future issue of this journal, but has not been fully edited. Content may change prior to final publication. Citation information: DOI 10.1109/TCOMM.2019.2937293, IEEE Transactions on Communications

symbols with higher magnitude. To see this, let us start from (1). For small ϕ_k, we can rewrite the observable y_k as

$$y_k \simeq x_k + j\phi_k x_k + w_k = x_k + (j\phi_k|x_k| + w'_k)\, e^{j\angle x_k} \quad (5)$$

$$= x_k + \underbrace{\mathcal{R}\{w'_k\}e^{j\angle x_k}}_{\text{radial noise}} + \underbrace{(\phi_k|x_k| + \mathcal{I}\{w'_k\})\, e^{j\left(\angle x_k + \frac{\pi}{2}\right)}}_{\text{angular noise}}, \quad (6)$$

where in (5) we have exploited the first order Taylor expansion $e^{j\phi_k} \simeq 1 + j\phi_k$, which is good if ϕ_k is small, and w'_k is statistically equivalent to w_k. We can distinguish two different noise components, a radial noise term, with variance $\sigma_w^2/2$, and an angular noise term, with variance

$$\mathrm{E}\left[(\phi_k|x_k| + \mathcal{I}\{w'_k\})^2\right] = \frac{\sigma_w^2}{2} + \sigma_\phi^2|x_k|^2 \quad (7)$$

$$= \frac{\sigma_w^2}{2}\left(1 + |x_k|^2\frac{2\sigma_\phi^2}{\sigma_w^2}\right) = \frac{\sigma_w^2}{2}\left(1 + f|x_k|^2\right), \quad (8)$$

where we have defined f as the ratio between the PN variance and the single-component AWGN variance. As we can see, the angular noise variance increases with the magnitude of the current symbol x_k. For this reason, a good constellation for a PN environment should increase the angular distance between points for increasing magnitude. We propose to design the spiral constellation in the presence of phase noise with the aim of maintaining a constant distance between consecutive laps, $D = 2\pi$, as derived in Theorem 1, and to increase the distance between the consecutive points according to the standard deviation of the angular noise term, which depends on the magnitude of the symbol. Hence, we define the new distance between consecutive points, on a spiral designed for a phase noise channel, as

$$D_m \simeq D\sqrt{1 + f_{\mathsf{s}}|c_m|^2}, \quad (9)$$

where the parameter f_{s} can be chosen according to the channel conditions. One possible choice is to set $f_{\mathsf{s}} = f$. On the other hand, we have observed that better results can be achieved by a further tuning of this parameter by considering a proper performance metric, as we will discuss in detail in the following sections. We define the parameters t_m, following Theorem 1,r with an extension according to (9), as

$$t_m = \sqrt{4\pi m\sqrt{1 + f_{\mathsf{s}}t_m^2}}, \quad (10)$$

which, solving for t_m^2, becomes

$$t_m^2 = \frac{(4\pi m)^2 f_{\mathsf{s}}}{2} + \sqrt{\frac{(4\pi m)^4 f_{\mathsf{s}}^2}{4} + (4\pi m)^2}. \quad (11)$$

Finally, by replacing the expressions for t_m in (3), we obtain the final expression for the constellation points. Notice that when $f_{\mathsf{s}} = 0$ the expressions for the points reduce to those we obtained in Section III-A. The important aspect to underline here is that the proposed constellations ensure a very simple design, being dependent on a single parameter, as opposed to other multilevel constellations usually adopted in communication systems, such as APSKs, whose design requires the optimization of multiple parameters, namely the number of rings, the number of constellation points per ring, the amplitude and phase rotation of each ring.

It is important to mention that the approximations adopted in this section are based on the assumption of large m, so they may not be totally accurate when m is small, that is, for the innermost constellation points. In particular, the first points of a spiral may not satisfy the property of constant distance D between them. It is in principle possible to overcome this problem by manually tweaking the positions of the first points, or by optimizing the starting value of m in eq. (3). We have verified that manually changing the starting point does not provide any information rate gain. This allows us to use eq. (3) without incurring in performance penalties and to maintain a simple and elegant expression for all constellation points.

IV. Performance Metrics

In this section, we describe the figures of merit that we will employ to evaluate the performance of the proposed constellations, with the aim of finding both theoretical and more practical results. Regarding the detection approach, we consider the detectors suitable for a PN scenario described in [24], based on different approximations of the received signal. Moreover, we also consider the optimal detector for the AWGN channel. These solutions are based on the principle of mismatched detection [25], which assumes the use of a properly selected auxiliary channel to approximate the real channel under consideration. If an optimal detector is available for the auxiliary channel, the results obtained represent a lower bound on the performance of the real channel, achievable with the considered detector.

A. Detection Strategies in the Presence of PN

Although an optimal detector for a channel affected by PN is impractical [9], [24], different possible detection strategies can be designed for a signal model defined as in (1), see for example [24] and references therein. As a first possibility, we can adopt a detector based on the low PN approximation already exploited to design the spiral constellation in (5)–(8), and proposed in [24]. However, we have verified that, for the scenarios considered in this paper, this low PN detector is outperformed by another detector, also proposed in [24], and based on a different approximation of the received signal. In the following, we report its derivation.

Let us start from the model (1). We can rewrite the observable y_k using an approximation which assumes a high signal-to-noise ratio (SNR) environment. The modulus of the observable can be expressed as

$$|y_k| = \left|x_k e^{j\phi_k} + w_k\right| \quad (12)$$

$$= \left||x_k|e^{j\angle x_k}e^{j\phi_k} + w'_k e^{j\angle x_k}e^{j\phi_k}\right| \quad (13)$$

$$= \left||x_k| + w'_k\right| \quad (14)$$

$$= \sqrt{\left(|x_k| + \mathcal{R}\{w'_k\}\right)^2 + \mathcal{I}\{w'_k\}^2} \quad (15)$$

$$\simeq |x_k| + \mathcal{R}\{w'_k\}. \quad (16)$$

The phase of the observable can be expressed as

$$\angle y_k = \angle\left(x_k e^{j\phi_k} + w_k\right) \quad (17)$$

$$= \angle\left(|x_k|e^{j\angle x_k}e^{j\phi_k} + w'_k e^{j\angle x_k}e^{j\phi_k}\right) \quad (18)$$

This article has been accepted for publication in a future issue of this journal, but has not been fully edited. Content may change prior to final publication. Citation information: DOI 10.1109/TCOMM.2019.2937293, IEEE Transactions on Communications

$$=\angle x_k + \phi_k + \angle\left(|x_k| + w'_k\right) \tag{19}$$

$$=\angle x_k + \phi_k + \tan^{-1}\frac{\mathcal{I}\{w'_k\}}{|x_k| + \mathcal{R}\{w'_k\}} \tag{20}$$

$$\simeq\angle x_k + \phi_k + \frac{\mathcal{I}\{w'_k\}}{|x_k|} + \ell\pi\,. \tag{21}$$

Eqs. (16) and (21) derive from a high SNR approximation. We now define the following auxiliary variables to perform detection:

$$u_k = |y_k| - |x_k| \tag{22}$$

$$v_k = |x_k|(\angle y_k - \angle x_k)_{\mathrm{mod}\,2\pi}\,, \tag{23}$$

where $|y_k|$ and $\angle y_k$ are defined in (16) and (21), respectively, and the operator $(\cdot)_{\mathrm{mod}\,2\pi}$ represents a wrapping of the phase in the interval $(0, 2\pi]$. Note that v_k, as defined above, represents the length of an arc of a circle corresponding to an angle equal to $(\angle y_k - \angle x_k)_{\mathrm{mod}\,2\pi}$ and, hence, the pair (u_k, v_k) represents a sufficient statistic for the detection of the observed sample y_k under the above mentioned high SNR assumption.

The likelihood function for the observation in the kth time instant (given x_k is transmitted) to be used for detection is a Gaussian probability density function (PDF) in the variables u_k and v_k, and can be expressed as [24]

$$f_{\text{hsnr}}(u_k, v_k|x_k) = \frac{1}{2\pi\sqrt{\frac{\sigma_w^2}{2}\left(\frac{\sigma_w^2}{2} + \sigma_\phi^2|x_k|^2\right)}}$$

$$\exp\left\{-\frac{1}{2}\left(\frac{u_k^2}{\frac{\sigma_w^2}{2}} + \frac{v_k^2}{\left(\frac{\sigma_w^2}{2} + \sigma_\phi^2|x_k|^2\right)}\right)\right\}, \tag{24}$$

and it represents the channel law we can use to design an optimal detector for the channel expressed by (16) and (21). The covariance matrix of the PDF (24) is

$$\mathbf{C}_k = \begin{bmatrix} \frac{\sigma_w^2}{2} & 0 \\ 0 & \frac{\sigma_w^2}{2} + \sigma_\phi^2|x_k|^2 \end{bmatrix}. \tag{25}$$

From (25), we can clearly see how PN affects the received sample only in the angular part, given by eq. (23), and that the angular noise variance increases with the squared magnitude of the transmitted symbol, $|x_k|^2$, while the variance of the radial noise is unaffected by x_k. We once again repeat that the detector based on the channel law (24) allows us to compute a lower bound to the capacity of the channel (1), which is achievable with this detection strategy. The approximations (16) and (21) are adopted only at the detector, as an auxiliary channel law, while the received sample y_k is always generated according to (1).

B. Reference Detector for the AWGN Channel

As a benchmark to compare the considered detection scheme, we will use an optimal detector for the AWGN channel, which is based on the following channel law

$$f_{\text{awgn}}(y_k|x_k) = \frac{1}{\pi\sigma_w^2}\exp\left\{-\frac{|y_k - x_k|^2}{\sigma_w^2}\right\}. \tag{26}$$

Notice that (26) is designed for the AWGN channel, and hence it does not take into account the presence of PN.

C. Figures of Merit

We use different figures of merit. The first performance metric is the achievable IR [26], computed numerically through the Monte Carlo technique described in [27]. According to mismatched detection, this measure represents a lower bound to the channel capacity, which is achievable with joint detection and decoding, computed without reference to any practical coding scheme. If we define by $\mathbf{x} = \{x_k\}_{k=0}^{K-1}$ a sequence of transmitted symbols, by $\mathbf{y} = \{y_k\}_{k=0}^{K-1}$ the corresponding received samples, and by $p(\mathbf{y}|\mathbf{x})$ the PDF of the selected auxiliary channel law, the lower bound on the achievable IR can be computed numerically as

$$I(\mathbf{x};\mathbf{y}) = \lim_{K\to\infty}\frac{1}{K}\mathrm{E}\left[\log_2\frac{p(\mathbf{y}|\mathbf{x})}{\sum_{\mathbf{x}'}p(\mathbf{y}|\mathbf{x}')P(\mathbf{x}')}\right], \tag{27}$$

where the summation at the denominator is performed over the M symbols of the constellations, and $P(\mathbf{x}')$ is the probability distribution of the transmitted symbols, in this paper equal to $1/M$ because the symbols are assumed to be equally likely. Moreover, we will consider the channel to be memoryless, hence (27) can be simplified by replacing the vector PDF with its scalar version $p(y_k|x_k)$, which is representative of a symbol-by-symbol detector. In this work, invoking the principle of mismatched detection [25], we set $p(y_k|x_k)$ equal to one of the described likelihood functions, $f_{\text{hsnr}}(y_k|x_k)$ or $f_{\text{awgn}}(y_k|x_k)$, to obtain a lower bound on the IR, achievable with the considered detectors. The parameter f_s of the spiral constellation can be chosen as the one providing the largest IR. More details on the optimization of f_s are reported in Appendix B.

We also consider an alternative theoretical measure, given by the pragmatic IR [28], [29]. This represents an upper bound to the IR achieved by a practical modulation and coding format (ModCod) following a *pragmatic* approach, that is, without iterations between detector and decoder. The pragmatic IR depends on the adopted bit-to-symbol mapping, which controls how transmitted bits are mapped on the complex constellation symbols. Therefore, we use this performance metric to optimize the parameter f_s given a particular bit-to-symbol mapping. The usual approach for PSKs and QAMs is Gray mapping, which ensures that adjacent constellation points differ by only one bit. APSKs usually adopt a quasi-Gray mapping, as they do not normally allow a fully Gray mapping. See for example those proposed in the DVB-S2X standard [2]. When the constellation is not regular, a good mapping has to be found through optimization as well, possibly jointly with the constellation points [30]. In the case of the spiral constellations proposed in this work, we observed that points tend to form branches. When the number of branches is $\sqrt{M}$, we propose to map the columns of symbols of QAM modulations to the branches of the spiral. More generally, if the number of branches is a power of 2, we can easily identify a transformation of the QAM symbols to map them into the branches of a spiral. In Fig. 2, we show an example of a spiral with $M = 256$ points and $f_\mathsf{s} = 0.00413$. We can clearly see how the points are arranged in 8 branches, each composed of 32 points; in this case, it is easy to adapt two columns of the 256 QAM mapping to each of the branches, in order to

This article has been accepted for publication in a future issue of this journal, but has not been fully edited. Content may change prior to final publication. Citation information: DOI 10.1109/TCOMM.2019.2937293, IEEE Transactions on Communications

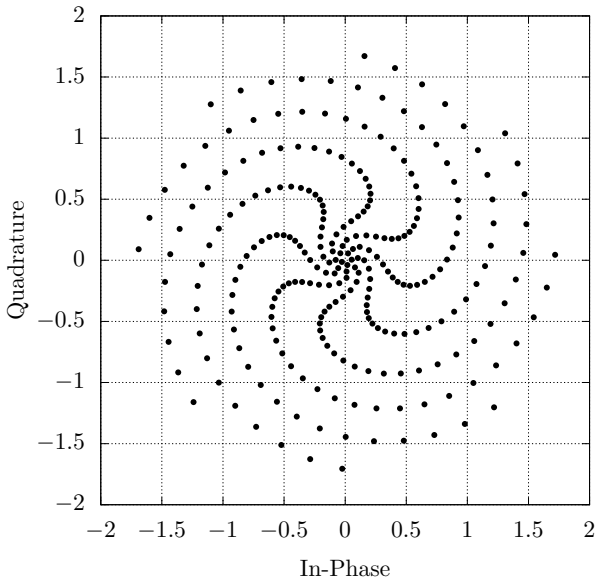

Figure 2. Spiral constellation with $M = 256$ points and $f_s = 0.00413$.

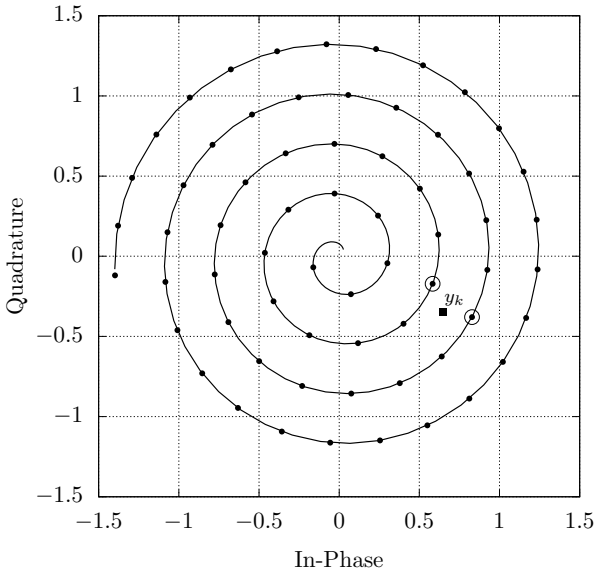

Figure 3. Example of reduced complexity detection on a spiral with $M = 64$ points and $f_s = 0$.

achieve a mapping that is Gray along each branch and between adjacent branches. We point out that spirals with a number of branches equal to a power of 2 are not necessarily optimal from an IR point of view. However, in order to avoid a complex optimization involving also the bit-to-symbol mapping, when we evaluate the pragmatic IR and the coded performance, we adopt only spirals with a number of branches equal to a power of 2. This further constraint is unnecessary, and not imposed, when using other performance metrics, like the achievable IR.

We will compare these theoretical bounds with a more practical measure, given by the IR achieved by real coded schemes. To this purpose, we will evaluate by computer simulation the packet error rate of coded transmissions based on one of the low-density parity-check (LDPC) codes defined by the DVB-S2X standard [2], which have excellent performance on the AWGN channel. In this case, we will use the parameter f_s optimized through the pragmatic IR.

As a last figure of merit, we also analyze the uncoded symbol error rate (SER) performance of the proposed solutions. While using long capacity-achieving codes (such as LDPC or turbo codes) is the solution for spectrally efficient communication systems, there are still reasons that make uncoded performance significant. In fact, for example, many receiver algorithms, such as clock recovery and equalization, work directly on the channel outputs. Moreover, in packet-oriented transmissions, the data is usually preceded by a fixed preamble marking the beginning of the packet and including information on the packet itself. This preamble cannot be coded, since the received stream cannot be decoded unless it is first partitioned into blocks. Another motivation is that in systems with extreme low-latency requirements, coding is not a feasible option.

V. Closest Points Search

In this section, we propose a low complexity detection approach that can be easily applied to the described spiral constellations. Let us assume that the observed sample is y_k, depicted with the square in the example reported in Fig. 3, which reports $M = 64$ points on a spiral in the form (2). Let us consider the equation for the constellation points (3). As we show below, it is now easy to find the two closest points on the spiral, highlighted with the circles in the figure. Our hypothesis is that one of these four points is also the maximum likelihood optimal point, which we validate numerically in Section VI-D.

We first notice that the closest point on a spiral $s(t)$ defined as in (2) must have the same phase value as y_k. Hence, the value of this point will be for $t = \angle y_k + n2\pi$, where n is unknown. In this point, the spiral has a magnitude of $|s(t)| = \angle y_k + n2\pi$.

We can now find the point on the spiral lap inside y_k, as $|y_k| \geq \angle y_k + n2\pi$, which gives us

$$n = \left\lfloor \frac{|y_k| - \angle y_k}{2\pi} \right\rfloor \text{ and } t_{\text{in}} = \angle y_k + 2\pi \left\lfloor \frac{|y_k| - \angle y_k}{2\pi} \right\rfloor . \quad (28)$$

It is easy to repeat this approach to find the closest point on the spiral lap outside y_k, getting $t_{\text{out}} = t_{\text{in}} + 2\pi$. Given these points on the spiral, we now want to find the constellation symbols near them. First, we solve the spiral (10) for m, to obtain

$$m = \frac{t_m^2}{4\pi\sqrt{1 + f_s t_m^2}} . \quad (29)$$

Replacing the values of t_{in} and t_{out} in (29), we can find the indexes of the closest constellation points, on the inner and outer laps, as

$$m_{\text{in}} = \left\lfloor \frac{t_{\text{in}}^2}{4\pi\sqrt{1 + f_s t_{\text{in}}^2}} \right\rceil \quad (30)$$

$$m_{\text{out}} = \left\lfloor \frac{t_{\text{out}}^2}{4\pi\sqrt{1 + f_s t_{\text{out}}^2}} \right\rceil , \quad (31)$$

where the operator $\lfloor a \rceil$ computes the closest integer to a. This entire procedure is reported in Fig. 4, a magnified version

This article has been accepted for publication in a future issue of this journal, but has not been fully edited. Content may change prior to final publication. Citation information: DOI 10.1109/TCOMM.2019.2937293, IEEE Transactions on Communications

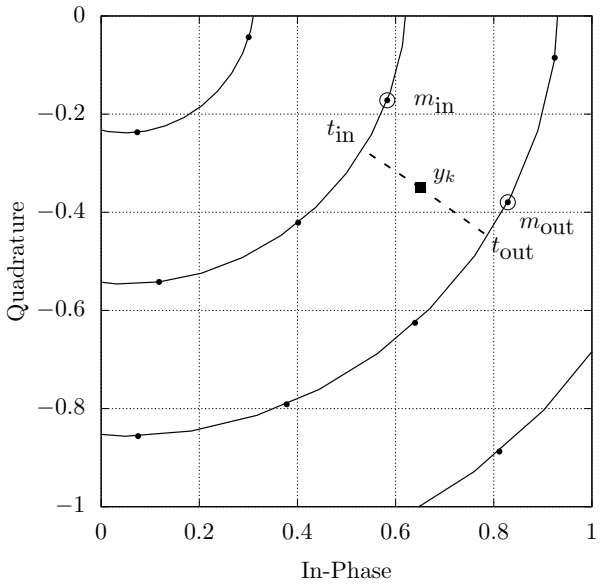

Figure 4. Points of the spiral closest to the observable.

of Fig. 3. We can then run a reduced complexity version of the detection algorithm, by evaluating the metrics (24) or (26) only on the identified two points of the constellation. This leads, particularly for high-order constellations, to a considerable complexity reduction. It is important to underline that the search of the closest points is made simple by the mathematical formulation of the constellation. In other cases, like APSK constellations from the DVB-S2X standard [2] or those obtained by means of more complex optimization strategies, this mathematical formulation is not available, and the closest points cannot be computed in a straightforward way. We also point out that the proposed closest point search approach is derived based only on the geometry of the spiral constellation, and it can be applied with any detection scheme.

VI. Numerical Results

In this section, we present a set of numerical results and simulations regarding the application of spiral constellations in the considered PN environment. As a means of comparison, we use the most commonly used multilevel modulation formats, namely QAM and APSK. For APSK, we adopt the ones proposed by the DVB-S2X standard [2], and the ones described in [31], which are designed to satisfy a Gray mapping. Using the same notation as in [31], a (m_1, m_2) Gray APSK constellation is composed of 2^{m_2} rings, each containing 2^{m_1} equally spaced points; in this paper, we adopt the options, among those listed in [31], which ensure the best performance in presence of PN, namely the $(4, 2)$ 64 Gray APSK and the $(4, 4)$ 256 Gray APSK. We also analyze the spiral QAM constellations proposed in [21], specifically designed for PN channels. We consider, as an application example, constellations with $M = 64$ and $M = 256$ points. This choice is dictated by the fact that multilevel constellations with medium-large sizes are one of the key solutions to deliver high transmission rates, a topic of great importance in present and future communication scenarios. It is also worth mentioning that PN is much more critical when the SNR is higher, that is, when multilevel constellations with large sizes are adopted by common communication standards. The whole analysis proposed in this paper can be easily applied to any constellation size. Indeed, we have performed the same kind of analysis for constellations with $M = 16$ points. For the sake of clarity, the results are not reported in the paper, but we will briefly comment on the performace in the next subsections.

All performance curves in this section are reported as a function of the ratio between the average energy per symbol and the thermal noise variance, E_{s}/N_0. We recall that, for the spiral constellations, an optimization is performed to select the best value of the parameter f_{s} for each E_{s}/N_0 value. This choice is justified by the fact that, in common adaptive coding and modulation (ACM) schemes, the modulation and coding formats are changed according to the channel conditions.

A. Achievable Information Rate

First of all, we want to assess the performance of spiral constellations on the AWGN channel, that is, when the observable is modeled as in (1), with $\sigma_\phi^2 = 0$. Fig. 5 shows the achievable IR comparison in this case, for $M = 64$ (Fig. 5 (a)) and $M = 256$ (Fig. 5 (b)). We can notice that the spiral designed with $f_{\mathsf{s}} = 0$ is essentially equivalent to QAM. On the other hand, an optimization of f_{s} can ensure theoretical gains up to almost 1 dB with respect to QAM constellations. The DVB-S2X APSKs show performance at the same level as the optimized spiral, except for small losses in the high SNR region, while Gray APSKs exhibit larger losses. Spiral QAMs exhibit performance comparable with the spiral with $f_{\mathsf{s}} = 0$. The same can be observed for constellations with $M = 16$ points. This first analysis tells us that a properly designed spiral can achieve, on the AWGN channel, a theoretical performance that is slightly better than that of other commonly adopted constellations.

We then consider the channel affected by PN. We use two values of PN variance, one relatively low, $\sigma_\phi^2 = 0.01$, representative of a well tracked PN, and one 10 times higher, $\sigma_\phi^2 = 0.1$, corresponding to a poor tracking performance. The results, in terms of achievable IR, are reported in Fig. 6.

Let us first consider the $\sigma_\phi^2 = 0.01$ case. We first notice that the detector for AWGN, unsurprisingly, exhibits very poor performance if associated with QAMs and APSKs, and also with spiral QAMs. In these curves, we can observe an effect that commonly arises when resorting to the mismatched detection framework. We can see that the curves decrease when the SNR increases. At medium-high SNR, PN tends to become the main impairment of the channel, while the adopted detector is designed for a completely different auxiliary channel model, the AWGN channel. Hence, in these regions, this detector is unable to work properly, since it does not represent a good approximation of the actual channel. Replacing the constellation with a suitable spiral, without changes at the receiver side, is sufficient to ensure a maximum achievable IR significantly higher than that achievable with the other constellations. The reference detector is clearly outperformed by the use of the alternative detection scheme, specifically

This article has been accepted for publication in a future issue of this journal, but has not been fully edited. Content may change prior to final publication. Citation information: DOI 10.1109/TCOMM.2019.2937293, IEEE Transactions on Communications

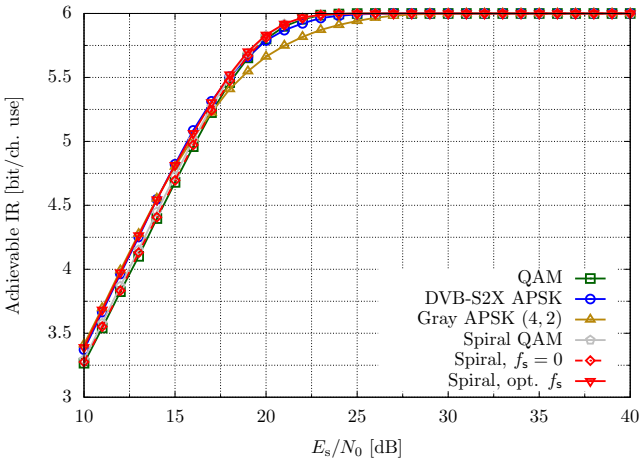

(a) $M = 64$, $\sigma_\phi^2 = 0$

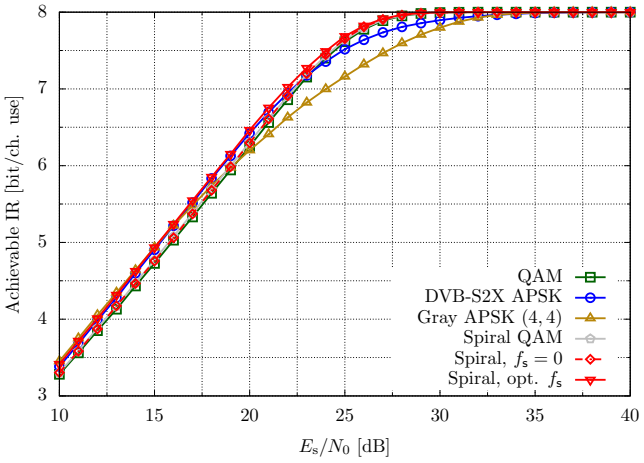

(b) $M = 256$, $\sigma_\phi^2 = 0$

Figure 5. Achievable IR on the AWGN channel for constellations with 64 and 256 points.

designed for a PN environment. By comparing the different constellation types, we see that spirals ensure significant gains over QAMs, and that the gaps increase with the SNR. For example, at 7 bit/ch. use (with $M = 256$), the gains are in the order of 3 dB. APSKs outperform QAMs in most SNR regions, but are generally inferior to spirals, with the exception of the 256 Gray APSK, which is comparable with the spiral almost everywhere. Spiral QAMs have performance similar to square QAMs. The curves tend to coincide around 10 dB, but it is worth to mention that an ACM scheme would probably adopt a lower constellation size in that SNR range, so the performance of higher order constellations is less relevant.

If we analyze the $\sigma_\phi^2 = 0.1$ case, instead, we see that spirals ensure much larger gains with respect to the other constellations. Also in this case, the best alternative is 256 Gray APSK, which, however, suffers large losses at high SNR. In this case we report only the curves obtained with the PN detector, since the AWGN detector is unable to work with this PN value.

We can also notice that most constellations are not robust enough to ensure that their achievable IR can reach the maximum theoretical value of $\log_2(M)$, even when the PN is relatively low. Instead, we show that a suitably designed constellation, like a spiral, can achieve $\log_2(M)$ bit/ch. use even in stronger PN conditions. If we consider constellations with $M = 16$ points, it is possible to show that, also in this case, a properly designed spiral can outperform other constellation types in all PN conditions. However, as could be easily foreseen, the possible gains are smaller, since 16-points constellations operate at lower SNR, where AWGN may be a more critical impairment than PN.

Finally, if we compare the results in Fig. 6 with the corresponding curves for the AWGN channel reported in Fig. 5, we see that the difference is significant, and the gaps increase with the SNR. This is not surprising as, when the SNR increases, PN becomes the main impairment of the channel. However, we can notice that spiral constellations are the solution which offers the best performance in terms of achievable IR in all channel conditions. These results show that the spiral QAM constellations proposed in [21] exhibit significant losses with respect to our proposed spirals in all PN conditions. This is mainly due to the lack of flexibility of their construction process, which does not allow an optimized design based on the PN conditions of the channel. Moreover, their design process does not allow for a simple mathematical formulation and, instead, relies on a more computationally intensive procedure. For these reasons, we will not consider them further.

B. Pragmatic Information Rate

Fig. 7 reports the pragmatic IR curves for the same cases as in Fig. 6, adopting only the detector for PN. For $\sigma_\phi^2 = 0.01$, we can notice that in the medium-low SNR range Gray APSKs provide the best performance, outperforming spirals and QAMs of at most 1 dB for $M = 64$ and 2 dB for $M = 256$. Also in this case, spirals outperform all alternatives at high SNR, for $M = 64$, and are comparable to the 256 Gray APSK. The loss of the spiral constellations is probably due to the suboptimality of the adopted bit-to-symbol mapping, and could be recovered with a more complex mapping obtained through optimization. For $\sigma_\phi^2 = 0.1$, spirals show extremely large gains starting from lower SNR values, so they certainly represent the desirable solution.

C. Coded Performance

In order to confirm these theoretical results, we have selected one of the LDPC codes from the DVB-S2X standard [2], with codeword size 64800 bits and rate $r = 5/6$. The results are reported in Table I, where the achieved IR (3rd column) is computed as $r \log_2 M$, and it represents the number of bits that can be effectively transferred in a single use of the channel. The SNR column of the table contains the value of E_s/N_0 needed to achieve a bit error rate (BER) of 10^{-6}. When this value is ∞, it means that the ModCod does not converge and that the BER never reaches low values. The table also reports the gaps of each ModCod from the corresponding achievable and pragmatic IR, and the peak to average power ratio (PAPR) of each constellation, which is another crucial measurement for wireless communications, where high power amplifiers are used. The values of f_s for the spiral constellations are those

This article has been accepted for publication in a future issue of this journal, but has not been fully edited. Content may change prior to final publication. Citation information: DOI 10.1109/TCOMM.2019.2937293, IEEE Transactions on Communications

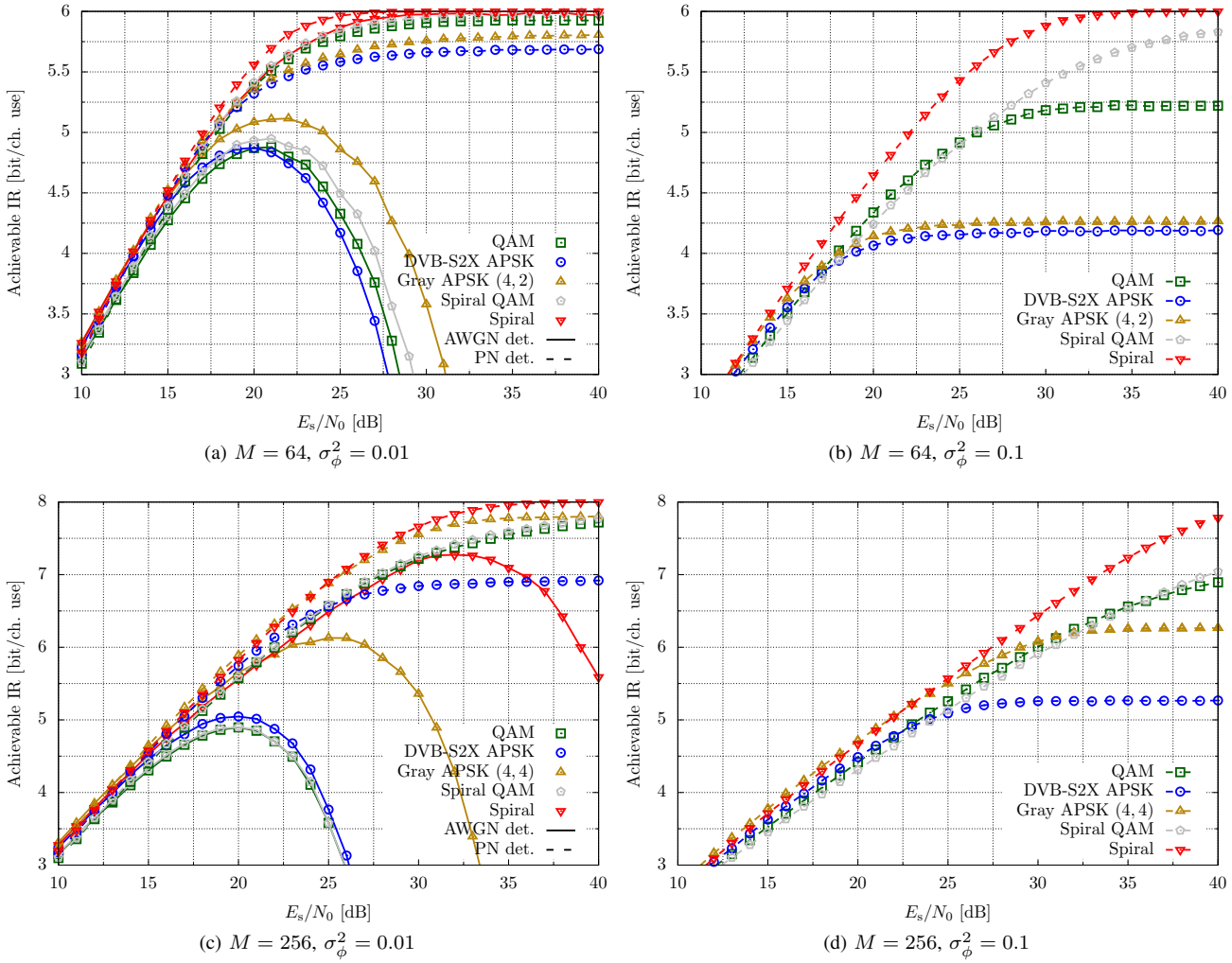

(a) $M = 64$, $\sigma_\phi^2 = 0.01$ (b) $M = 64$, $\sigma_\phi^2 = 0.1$

(c) $M = 256$, $\sigma_\phi^2 = 0.01$ (d) $M = 256$, $\sigma_\phi^2 = 0.1$

Figure 6. Achievable IR on the channels affected by PN, for constellations with 64 and 256 points.

selected by means of the technique described in Section IV. By analyzing the table, we see that the results are perfectly in line with what foreseen by the pragmatic IR. In particular, if we look at the $\sigma_\phi^2 = 0.01$ case, we see that the 64 Gray APSK exhibits a 0.4 dB gain over the spiral, with a comparable PAPR, and that both QAM and DVB-S2X APSK have a lower PAPR and slightly worse performance, comparable to that of the spiral. For $M = 256$, instead, the Gray APSK shows a 0.9 dB performance gain with respect to the spiral, with a 0.65 dB higher PAPR. Both the QAM and the DVB-S2X APSK show poor convergence in this case. In the $\sigma_\phi^2 = 0.1$, on the other hand, spiral constellations are the only solution which is able to converge, for both $M = 64$ and $M = 256$, and that the gaps from the corresponding pragmatic IR are not excessive, despite the fact that the adopted code has been specifically optimized for the AWGN channel. Notice that the constellation reported in Fig. 2 is used in this case.

D. Uncoded Symbol Error Rate

Finally, we assess the performance in case of uncoded transmission. In Fig. 8, we report the uncoded SER performance for constellations with 256 points. Similar results have been obtained for $M = 64$, not reported here due to the lack of space. The first thing we notice is the poor performance of APSKs even on the AWGN channel ($\sigma_\phi^2 = 0$), where QAM and spiral are almost equivalent. When PN affects the channel,[1] APSKs and QAM do not converge. Instead, the spiral constellation offers satisfactory performance. Regarding the selection of the parameter f_s, the values optimizing the pragmatic IR are the same which are also optimal for the SER. The optimized values for the achievable IR, instead, coincide with the other two cases only at high SNR, while they tend to be lower for low SNR values.

Fig. 9 shows the same uncoded SER results for spiral constellations, but it includes also the reduced complexity strategy proposed in Section V. For these results, we operate the detector on the two closest points, as reported in Fig. 4, achieving a complexity reduction of a factor $M/2 = 128$, for a 256 points constellation. We see that the detector running on the two closest points achieves exactly the same performance as the detector evaluating the value of the metric (24) on all the constellation points, in both PN scenarios. This shows that 2 points are sufficient to achieve optimal performance

[1]In presence of PN, the detector for AWGN does not converge at all, for any constellation. For this reason, the corresponding curves are not reported in the figures.

This article has been accepted for publication in a future issue of this journal, but has not been fully edited. Content may change prior to final publication. Citation information: DOI 10.1109/TCOMM.2019.2937293, IEEE Transactions on Communications

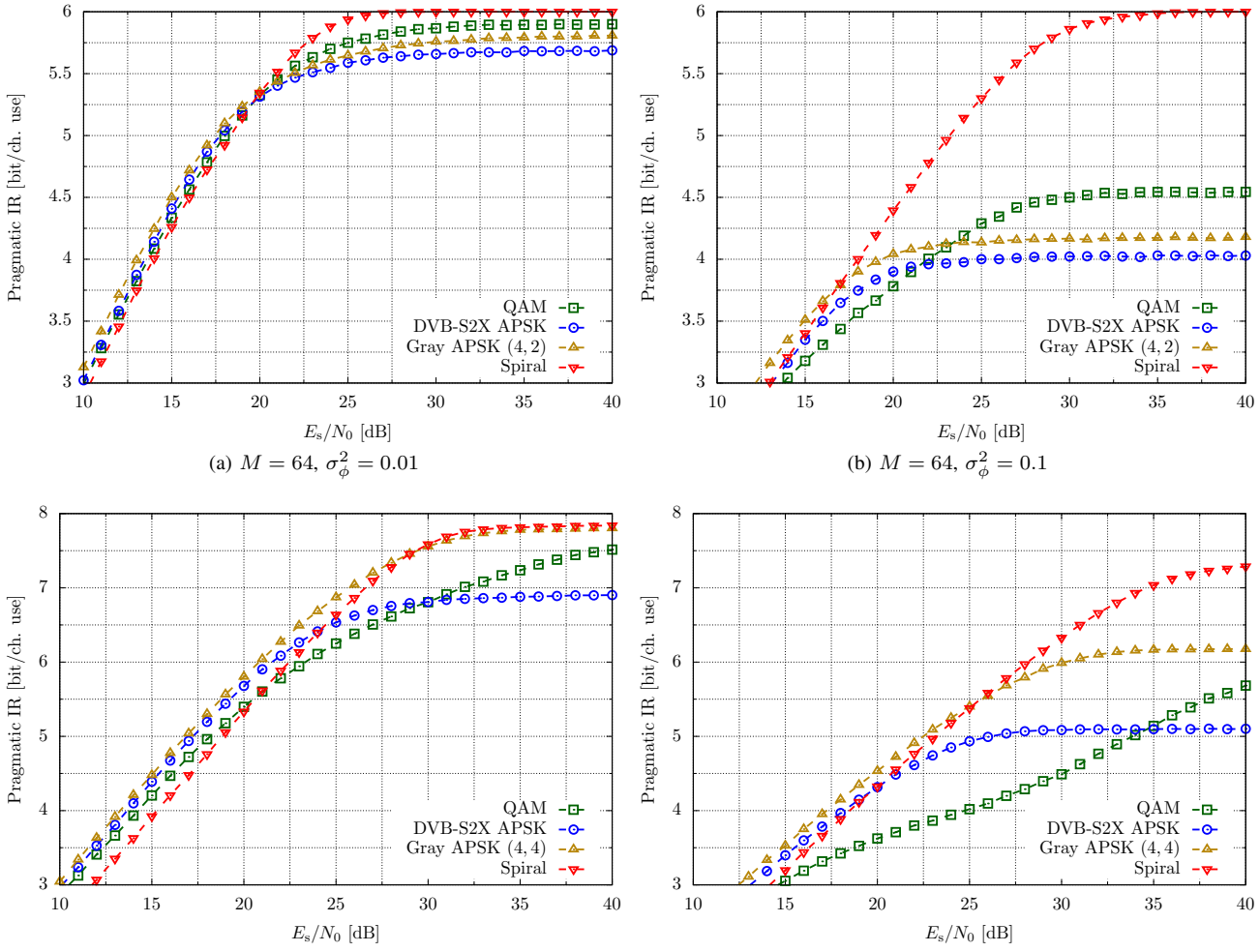

(a) $M = 64$, $\sigma_\phi^2 = 0.01$ (b) $M = 64$, $\sigma_\phi^2 = 0.1$

(c) $M = 256$, $\sigma_\phi^2 = 0.01$ (d) $M = 256$, $\sigma_\phi^2 = 0.1$

Figure 7. Pragmatic IR on the channels affected by PN, for constellations with 64 and 256 points.

Table I
CODED PERFORMANCE.

			$\sigma_\phi^2 = 0.01$				$\sigma_\phi^2 = 0.1$			
M	PAPR [dB]	IR	SNR [dB]	Gap from A. IR [dB]	Gap from P. IR [dB]	f_s (spirals)	SNR [dB]	Gap from A. IR [dB]	Gap from P. IR [dB]	f_s (spirals)
QAM										
64	5.02	5.00	19.72	1.86	1.69	-	∞	-	-	-
256	5.07	6.67	32.39	6.65	3.88	-	∞	-	-	-
DVB-S2X APSK										
64	5.15	5.00	19.63	2.06	1.88	-	∞	-	-	-
256	5.21	6.67	∞	-	-	-	∞	-	-	-
Gray APSK										
64	5.48	5.00	19.34	1.95	1.87	-	∞	-	-	-
256	6.12	6.67	25.94	2.12	2.02	-	∞	-	-	-
Spiral										
64	5.45	5.00	19.72	2.66	1.37	0.00413	24.87	2.76	1.66	0.01830
256	5.47	6.67	26.84	2.93	1.70	0.00112	34.98	3.57	2.93	0.00413

This article has been accepted for publication in a future issue of this journal, but has not been fully edited. Content may change prior to final publication. Citation information: DOI 10.1109/TCOMM.2019.2937293, IEEE Transactions on Communications

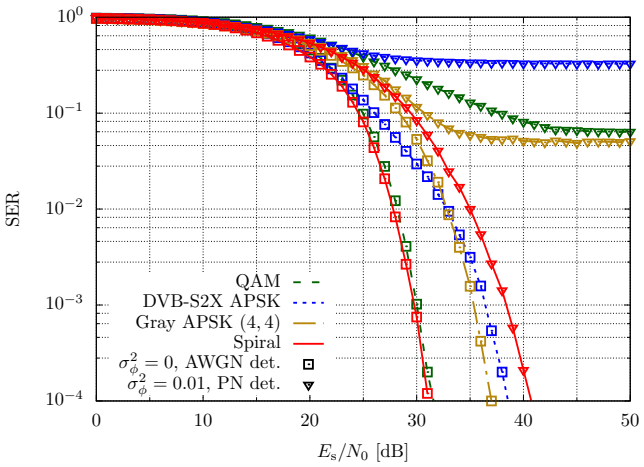

(a) $M = 256$, $\sigma_\phi^2 = 0.01$

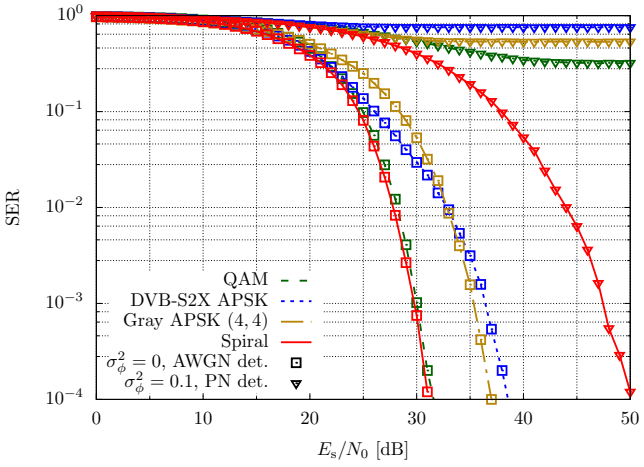

(b) $M = 256$, $\sigma_\phi^2 = 0.1$

Figure 8. Uncoded SER for constellations with $M = 256$ points.

in this scenario. It is worth mentioning that the closest point search can be beneficial also to reduce the complexity of coded performance. However, LDPC codes are powerful channel coding schemes, which achieve quasi-error-free performance at much lower SNR values with respect to uncoded transmission (compare, for example, the SNR values in Table I with the curves in Fig. 8). For this reason, limiting the search to only the two closest points is not a feasible solution, as the additive noise level is too high to be reasonably certain to find the correct point close to the received sample. Increasing the size of the constellation subset, instead, can ensure very good performance, although with a more limited complexity reduction with respect to the uncoded case.

VII. Conclusions

We have proposed new spiral constellations, specifically designed for phase noise channels. The points of the new constellations are described by an elegant analytical form, that allows an extremely simple design. In terms of performance, they outperform other competing constellations for a large range of SNR, especially in harsh phase noise conditions. Moreover, we have shown that they allow to achieve high information rate, close to 8 bits per channel use, and they are

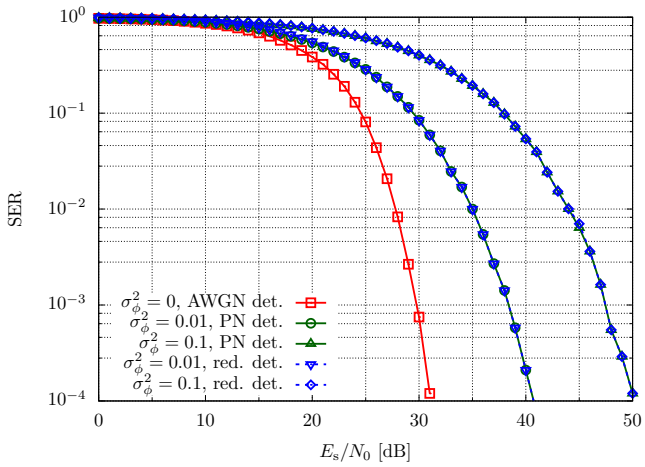

Figure 9. Uncoded SER for spiral constellations with $M = 256$ points and the reduced complexity detector.

suitable for application in practical coded systems adopting state-of-the-art channel codes, without the need for a redesign of the code.

Appendix A
Proof of Theorem 1

Proof: We can compute the distance D_m in (4) as

$$D_m = \left| t_{m+1} e^{j t_{m+1}} - t_m e^{j t_m} \right| \tag{32}$$

$$= \left| t_m e^{j t_m} \right| \left| \frac{t_{m+1}}{t_m} e^{j(t_{m+1} - t_m)} - 1 \right| \tag{33}$$

$$= \sqrt{2Dm} \left| \sqrt{1 + \frac{1}{m}} e^{j\left(\sqrt{2D(m+1)} - \sqrt{2Dm}\right)} - 1 \right| \tag{34}$$

$$\simeq \sqrt{2Dm} \left| \left(1 + \frac{1}{2m}\right) \cdot \left[1 + j\left(\sqrt{2D(m+1)} - \sqrt{2Dm}\right)\right] - 1 \right| \tag{35}$$

$$= \sqrt{2Dm} \left| j \left(1 + \frac{1}{2m}\right) \cdot \left(\sqrt{2D(m+1)} - \sqrt{2Dm}\right) + \frac{1}{2m} \right| \tag{36}$$

$$= 2Dm \left| j \left(\sqrt{1 + \frac{1}{m}} - 1 \right) \left(1 + \frac{1}{2m}\right) + \frac{1}{2m\sqrt{2Dm}} \right| \tag{37}$$

$$\simeq 2Dm \left| \frac{j}{2m} \left(1 + \frac{1}{2m}\right) + \frac{1}{2m\sqrt{2Dm}} \right| \tag{38}$$

$$= D \left| j + \frac{j}{2m} + \frac{1}{\sqrt{2Dm}} \right| \simeq D\,, \tag{39}$$

where (34) is computed by replacing the expression for the constellation points, $t_m = \sqrt{2Dm}$, (35) is obtained expressing the square root and the exponential through a Taylor series, (38) is also computed by means of a Taylor series expansion of the square root, and (39) derives from the assumption of a large value of m. In general, all the involved approximations are accurate if m is sufficiently large and the difference $t_{m+1} - t_m$ is sufficiently small, which again happens if m is sufficiently

This article has been accepted for publication in a future issue of this journal, but has not been fully edited. Content may change prior to final publication. Citation information: DOI 10.1109/TCOMM.2019.2937293, IEEE Transactions on Communications

large. Now, we also want the laps of the spiral (perpendicular to the spiral) to be at the same distance D as the distances along the spiral. So, if we move a full lap, the magnitude should be increased by D, according to the following equation,

$$\left|(t+2\pi)e^{j(t+2\pi)}\right| = \left|te^{jt}\right| + D\,, \tag{40}$$

from which $D = 2\pi$ follows. For small values of m, the distances between points deviate slightly from the desired constant 2π. It is easy to verify that, if $m \geq 9$, the error on the distance due to the adopted approximation is below 1%, and it quickly decreases as m becomes larger. The final expression for placing the points is then $t_m = \sqrt{4\pi m}$. This definition approximately leads to constant distances 2π between consecutive points along the spiral and between consecutive laps of the spiral. ■

APPENDIX B
OPTIMIZATION OF f_s

Formally, we select the optimal value of f_s as

$$f_\mathsf{s}^* = \arg\max_{f_\mathsf{s}} I(f_\mathsf{s})\,, \tag{41}$$

where I is the bound on the achievable IR, computed as in (27), in which we have explicitly shown the dependence on the adopted constellation, defined by the parameter f_s. In order to narrow down the search domain for f_s, we observe that it is convenient to place the points on consecutive laps of the spiral in such a way that points on the two laps are not aligned in phase with each other; this ensures a larger distance between the points, and it is more critical for the outermost laps of the spiral, where more points are placed. We start from (11), which defines how the points are placed along the spiral. For the most external lap of the spiral, indexed by the largest values of m, (11) can be approximated as

$$t_m^2 \simeq (4\pi m)^2 f_\mathsf{s}\,, \tag{42}$$

from which

$$t_m \simeq 4\pi m\sqrt{f_\mathsf{s}}\,. \tag{43}$$

We define by $M_{\rm out}$ the number of points on the outermost lap of the spiral. From (3), the last point of the spiral is

$$c_M = t_M e^{jt_M}\,. \tag{44}$$

According to our previous observation, we impose the phase of the last point to be approximately half way between those of the two nearest point on the inner lap, $c_{M-M_{\rm out}}$ and $c_{M-M_{\rm out}-1}$, so the phase of c_M can be computed as

$$\angle c_M = \frac{1}{2}(\angle c_{M-M_{\rm out}} + \angle c_{M-M_{\rm out}-1}) + 2\ell\pi \tag{45}$$

where the term $+2\ell\pi$ takes into account the inherent periodicity of the phases. From (43), we have that

$$\angle c_M = t_M \simeq 4\pi M\sqrt{f_\mathsf{s}} \tag{46}$$

$$\angle c_{M-M_{\rm out}} = t_{M-M_{\rm out}} \simeq t_M - 4\pi M_{\rm out}\sqrt{f_\mathsf{s}} \tag{47}$$

$$\angle c_{M-M_{\rm out}-1} = t_{M-M_{\rm out}-1} \simeq t_M - 4\pi M_{\rm out}\sqrt{f_\mathsf{s}} - 4\pi\sqrt{f_\mathsf{s}}\,. \tag{48}$$

By replacing (46)–(48) in (45) and setting $\ell = 1$, we get

$$t_m = 2\pi + t_m - 4\pi M_{\rm out}\sqrt{f_\mathsf{s}} - 2\pi\sqrt{f_\mathsf{s}}\,, \tag{49}$$

from which we obtain

$$f_\mathsf{s} = \frac{1}{(2M_{\rm out}+1)^2}\,. \tag{50}$$

Eq. (50) gives us a set of possible values of f_s, which depend on the number of points on the outermost lap of the spiral. For example, for $M_{\rm out} \in [8, 15]$, we obtain that good values of f_s belong to the set

$$[3.46 \;\; 2.77 \;\; 2.27 \;\; 1.89 \;\; 1.60 \;\; 1.37 \;\; 1.19 \;\; 1.04] \times 10^{-3}\,. \tag{51}$$

The maximization in (41) is then performed on this set of values of f_s, and a fine search is subsequently carried out around the value of f_s which ensures the maximum IR.

REFERENCES

[1] A. Hajimiri and T. H. Lee, "A general theory of phase noise in electrical oscillators," *IEEE Journal of Solid-State Circuits*, vol. 33, pp. 179–194, Feb 1998.

[2] ETSI EN 302 307-2 Digital Video Broadcasting (DVB), Second generation framing structure, channel coding and modulation systems for Broadcasting, Interactive Services, News Gathering and other broadband satellite applications, Part II: S2-Extensions (DVB-S2X). Available on ETSI web site (http://www.etsi.org).

[3] G. Durisi, A. Tarable, C. Camarda, R. Devassy, and G. Montorsi, "Capacity bounds for MIMO microwave backhaul links affected by phase noise," *IEEE Transactions on Communications*, vol. 62, pp. 920–929, March 2014.

[4] G. Colavolpe, T. Foggi, E. Forestieri, and G. Prati, "Robust multilevel coherent optical systems with linear processing at the receiver," *J. Lightwave Technol.*, vol. 27, pp. 2357–2369, Jul 2009.

[5] H. Meyr, M. Moeneclaey, and S. A. Fechtel, *Digital communication receivers*. John Wiley & Sons, 1998.

[6] U. Mengali and A. N. D'Andrea, *Synchronization Techniques for Digital Receivers (Applications of Communications Theory)*. Plenum Press, 1997.

[7] G. Colavolpe, "Communications over phase-noise channels: A tutorial review," in *2012 6th Advanced Satellite Multimedia Systems Conference (ASMS) and 12th Signal Processing for Space Communications Workshop (SPSC)*, pp. 316–327, Sep. 2012.

[8] G. Colavolpe and R. Raheli, "Noncoherent sequence detection," *IEEE Trans. Commun.*, vol. 47, pp. 1376–1385, Sept. 1999.

[9] G. Colavolpe, A. Barbieri, and G. Caire, "Algorithms for iterative decoding in the presence of strong phase noise," *IEEE J. Select. Areas Commun.*, vol. 23, pp. 1748–1757, Sept. 2005.

[10] C. Herzet, N. Noels, V. Lottici, H. Wymeersch, M. Luise, M. Moeneclaey, and L. Vandendorpe, "Code-aided turbo synchronization," *Proceedings of the IEEE*, vol. 95, pp. 1255–1271, June 2007.

[11] A. Barbieri and G. Colavolpe, "Soft-output decoding of rotationally invariant codes over channels with phase noise," *IEEE Trans. Commun.*, vol. 55, pp. 2125–2133, Nov. 2007.

[12] A. Barbieri and G. Colavolpe, "Simplified soft-output detection of CPM signals over coherent and phase noise channels," *IEEE Trans. Wireless Commun.*, vol. 6, pp. 2486–2496, July 2007.

[13] M. Nissila and S. Pasupathy, "Adaptive iterative detectors for phase-uncertain channels via variational bounding," *IEEE Trans. Commun.*, vol. 57, pp. 716–725, Mar. 2009.

[14] A. Piemontese, N. Mazzali, and G. Colavolpe, "Improving the spectral efficiency of FDM-CPM systems through packing and multiuser processing," *International Journal of Satellite Communications and Networking*, vol. 30, pp. 62 – 72, Feb. 2012.

[15] R. Combes and S. Yang, "An approximate ML detector for MIMO channels corrupted by phase noise," *IEEE Transactions on Communications*, vol. 66, pp. 1176–1189, March 2018.

[16] X. Yang, S. Jin, and C. Wen, "Symbol detection of phase noise-impaired massive MIMO using approximate bayesian inference," *IEEE Signal Processing Letters*, vol. 26, pp. 607–611, April 2019.

[17] G. Foschini, R. Gitlin, and S. Weinstein, "On the selection of a two-dimensional signal constellation in the presence of phase jitter and Gaussian noise," *Bell System Tech. J.*, vol. 52, pp. 927–965, July 1973.

[18] F. Kayhan and G. Montorsi, "Constellation design for memoryless phase noise channels," *IEEE Trans. Wireless Commun.*, vol. 13, pp. 2874–2883, May 2014.

[19] R. Krishnan, A. Graell i Amat, T. Eriksson, and G. Colavolpe, "Constellation optimization in the presence of strong phase noise," *IEEE Trans. Commun.*, vol. 61, pp. 5056–5066, Dec. 2013.

[20] M. A. Tariq, H. Mehrpouyan, and T. Svensson, "Performance of circular QAM constellations with time varying phase noise," in *Proc. IEEE International Symposium on Personal, Indoor, and Mobile Radio Commun.*, (Sydney, Australia), pp. 2365–2370, Sept. 2012.

[21] B. J. Kwak, N. O. Song, B. Park, and D. S. Kwon, "Spiral QAM: A novel modulation scheme robust in the presence of phase noise," in *Proc. Vehicular Tech. Conf.*, (Calgary, BC, Canada), Sept. 2008.

[22] T. Minowa, H. Ochiai, and H. Imai, "Phase-noise effects on turbo trellis-coded over M-ary coherent channels," *IEEE Transactions on Communications*, vol. 52, pp. 1333–1343, Aug 2004.

[23] J. Proakis and M. Salehi, *Digital Communications*. McGraw-Hill, 5th ed., 2008.

[24] R. Krishnan, M. R. Khanzadi, T. Eriksson, and T. Svensson, "Soft metrics and their performance analysis for optimal data detection in the presence of strong oscillator phase noise," *IEEE Trans. Commun.*, vol. 61, pp. 2385–2395, June 2013.

[25] N. Merhav, G. Kaplan, A. Lapidoth, and S. Shamai, "On information rates for mismatched decoders," *IEEE Trans. Inform. Theory*, vol. 40, pp. 1953–1967, Nov. 1994.

[26] T. M. Cover and J. A. Thomas, *Elements of Information Theory*. New York: John Wiley & Sons, 2nd ed., 2006.

[27] D. M. Arnold, H.-A. Loeliger, P. O. Vontobel, A. Kavčić, and W. Zeng, "Simulation-based computation of information rates for channels with memory," *IEEE Trans. Inform. Theory*, vol. 52, pp. 3498–3508, Aug. 2006.

[28] J. B. Soriaga, H. Pfister, and P. Siegel, "Determining and approaching achievable rates of binary intersymbol interference channels using multistage decoding," *IEEE Trans. Inform. Theory*, vol. 53, pp. 1416–1429, Apr. 2007.

[29] G. Caire, G. Taricco, and E. Biglieri, "Bit-interleaved coded modulation," *IEEE Trans. Inform. Theory*, vol. 44, pp. 927–946, May 1998.

[30] F. Kayhan and G. Montorsi, "Joint signal-labeling optimization under peak power constraint," *Intern. J. of Satellite Communications and Networking*, vol. 30, pp. 251–263, Nov./Dec. 2012.

[31] Z. Liu, Q. Xie, K. Peng, and Z. Yang, "APSK constellation with Gray mapping," *IEEE Commun. Letters*, vol. 15, pp. 1271–1273, Dec. 2011.

Alessandro Ugolini was born in Parma, Italy, in 1987. He received the master's degree in Telecommunications Engineering (cum laude) from the University of Parma in 2012, and the Ph.D. degree in Information Technology from the same University in 2016. In 2012 he was awarded a National Inter-University Consortium for Telecommunications (CNIT) grant and a research grant funded by the Department of Information Engineering (DII), University of Parma, for the study of synchronization algorithms for spectrally efficient systems. In 2016 he has been a postdoctoral researcher at the DII. In 2017 he has been visiting researcher at the Department of Electrical Engineering at Chalmers University of Technology, Gothenburg, Sweden, and at Interdisciplinary Centre for Security, Reliability and Trust, University of Luxembourg. He received the best paper award at the IEEE Wireless Communications and Networking Conference (WCNC 2019). Since 2017 he is a researcher at the Department of Engineering and Architecture (DIA) of the University of Parma. His main research interests include digital communications, applied information theory and synchronization.

Amina Piemontese (S'09–M'11) was born in San Giovanni Rotondo, Italy, in 1980. She received the Dr.Ing. degree in Telecommunications Engineering from the University of Parma, Italy, in 2006 and the Ph.D. degree in Information Technology from the University of Parma and from TELECOM Bretagne, Brest, France, in 2011. From 2011 to April 2015 she held a postdoctorate position at the Department of Information Engineering of the University of Parma. In May 2015 she joined the Department of Electrical Engineering at Chalmers University of Technology, Gothenburg, Sweden, where now she is a researcher. Her research activity includes various topics in digital communications, with particular emphasis on iterative joint detection and decoding algorithms, multiuser communications theory and coding for distributed storage. She received the best paper award at the 5th Advanced Satellite Mobile Systems Conference and 11th International Workshop on Signal Processing for Space Communications (ASMS&SPSC 2010) and at the IEEE Wireless Communications and Networking Conference (WCNC), and the Marie Curie Individual Fellowship of the European Commission.

Thomas Eriksson received the Ph.D. degree in Information Theory from Chalmers University of Technology, Gothenburg, Sweden, in 1996. From 1990 to 1996, he was at Chalmers. In 1997 and 1998, he was at AT&T Labs - Research, Murray Hill, NJ, USA. In 1998 and 1999, he was at Ericsson Radio Systems AB, Kista, Sweden. Since 1999, he has been with Chalmers University, where he is currently a professor of communication systems. Further, he was a guest professor with Yonsei University, S. Korea, in 2003-2004. He has authored or co-authored more than 250 journal and conference papers, and holds 14 patents. Prof. Eriksson is leading the research on hardware-constrained communications with Chalmers University of Technology. His research interests include communication, data compression, and modeling and compensation of non-ideal hardware components (e.g. amplifiers, oscillators, and modulators in communication transmitters and receivers, including massive MIMO). Currently, he is leading several projects on e.g. 1) massive MIMO communications with imperfect hardware, 2) MIMO communication taken to its limits: 100Gbit/s link demonstration, 3) mm-Wave MIMO testbed design, 4), Satellite communication with phase noise limitations, 5) Efficient and linear transceivers, etc. He is currently the Vice Head of the Department of Signals and Systems with Chalmers University of Technology, where he is responsible for undergraduate and master´s education.